Diabetologia (2013) 56:2713–2722
DOI 10.1007/s00125-013-3053-3

ARTICLE

PREP1 deficiency downregulates hepatic lipogenesis and attenuates steatohepatitis in mice

Francesco Oriente · Serena Cabaro · Antonietta Liotti · Michele Longo · Luca Parrillo · Teresa Bruna Pagano · Gregory Alexander Raciti · Dmitry Penkov · Orlando Paciello · Claudia Miele · Pietro Formisano · Francesco Blasi · Francesco Beguinot

Received: 19 June 2013 / Accepted: 26 August 2013 / Published online: 20 September 2013

Abstract
Aims/hypothesis The aim of this study was to investigate the function of *Prep1* (also known as *Pknox1*) in hepatic lipogenesis.
Methods The hepatic lipogenesis pathway was evaluated by real-time RT-PCR and Western blot. Biochemical variables were assessed using a clinical chemistry analyser.
Results Serum triacylglycerols and liver expression of fatty acid synthase (FAS) were significantly decreased in *Prep1* hypomorphic heterozygous (*Prep1*$^{i/+}$) mice compared with their non-hypomorphic littermates. Upstream FAS expression, phosphorylation of protein kinase C (PKC)ζ, liver kinase B1 (LKB1), AMP-activated protein kinase (AMPK) and acetyl-CoA carboxylase (ACC) increased in *Prep1*$^{i/+}$ mice, while protein and mRNA levels of the lipid phosphatase inhibitor of PKCζ, SH2-containing inositol 5′-phosphatase 2 (SHIP2), was more than 60% reduced. Consistent with these findings, HepG2 cells transfected with *Prep1* cDNA exhibited increased triacylglycerol accumulation and FAS expression, with strongly reduced PKCζ, LKB1, AMPK and ACC phosphorylation. Further experiments revealed the presence of both *Prep1* and its major partner *Pbx1* at the *Ship2* (also known as *Inppl1*) promoter. PBX-regulating protein 1 (PREP1) and pre-B cell leukaemia transcription factor 1 (PBX1) enhanced *Ship2* transcription. The PREP1$_{HR}$ mutant, which is unable to bind PBX1, exhibited no effect on *Ship2* function, indicating transcriptional activation of *Ship2* by the PREP1/PBX1 complex. Treatment with a methionine- and choline-deficient diet (MCDD) induced steatosis in both *Prep1*$^{i/+}$ and non-hypomorphic control mice. However, alanine aminotransferase increase, intracellular triacylglycerol content and histological evidence of liver steatosis, inflammation and necrosis were significantly less evident in *Prep1*$^{i/+}$ mice, indicating that *Prep1* silencing protects mice from MCDD-induced steatohepatitis.
Conclusions/interpretation Our results indicate that *Prep1* silencing reduces lipotoxicity by increasing PKCζ/LKB1/AMPK/ACC signalling, while levels of PREP1 expression may determine the risk of steatohepatitis and its progression.

Keywords AMPK · Lipogenesis · PBX1 · PREP1 · SHIP2 · Steatohepatitis

Abbreviations

ACC	Acetyl-CoA carboxylase
ALT	Alanine aminotransferase
AMPK	AMP-activated protein kinase
CAMKKβ	Calcium/calmodulin-dependent protein kinase kinase β
ChIP	Chromatin immunoprecipitation
FAS	Fatty acid synthase
HepG2	Human hepatocellular carcinoma
LKB1	Liver kinase B1
MCDD	Methionine- and choline-deficient diet

Francesco Oriente and Serena Cabaro contributed equally to this study.

Electronic supplementary material The online version of this article (doi:10.1007/s00125-013-3053-3) contains peer-reviewed but unedited supplementary material, which is available to authorised users.

F. Oriente · S. Cabaro · A. Liotti · M. Longo · L. Parrillo · G. A. Raciti · C. Miele · P. Formisano · F. Beguinot (✉)
Department of Translational Medical Sciences, 'Federico II' University of Naples and Institute of Experimental Endocrinology and Oncology, National Council of Research,
Via Pansini 5, 80131 Naples, Italy
e-mail: beguino@unina.it

T. B. Pagano · O. Paciello
Department of Veterinary Medicine and Animal Production, 'Federico II' University of Naples, Naples, Italy

D. Penkov · F. Blasi
IFOM (FIRC Institute of Molecular Oncology), Milan, Italy

D. Penkov
Moscow State University, Moscow, Russia

NAFLD	Non-alcoholic fatty liver disease
NASH	Non-alcoholic steatohepatitis
ORO	Oil Red O
PBX	Pre-B cell leukaemia transcription factor
PKA	Protein kinase A
PKC	Protein kinase C
PREP1	PBX-regulating protein 1
SHIP2	SH2-containing inositol 5′-phosphatase 2
SREBP	Sterol regulatory element binding protein
TG	Triacylglycerol
WT	Wild-type

Introduction

The liver has a very important role in lipid homeostasis and metabolism [1]. In the liver, an excess of carbohydrates results in insulin-dependent de novo fatty acid synthesis. This effect is largely accomplished through the downregulation of AMP-activated protein kinase (AMPK) [2]. Indeed, AMPK phosphorylates and inactivates acetyl-CoA carboxylase (ACC), inhibiting fatty acid biosynthesis [3, 4]. AMPK activation requires phosphorylation at Thr172 by one or more upstream kinases, including liver kinase B1 (LKB1) [5, 6].

In addition to the de novo synthesis of fatty acids, however, other events can cause the intrahepatic accumulation of lipids, including increased lipid uptake, impaired lipoprotein secretion or synthesis and reduced fatty acid oxidation [7]. Insulin resistance can impact on several of these processes, leading to excess liver fat deposition and non-alcoholic fatty liver disease (NAFLD). NAFLD, in turn, facilitates oxidative hepatocellular damage, inflammation and activation of fibrogenesis. The resulting non-alcoholic steatohepatitis (NASH) can progress towards cirrhosis and hepatocellular carcinoma. NAFLD represents the most common liver disease and the leading cause of altered liver enzymes in Western countries [8]. Its development parallels that of insulin resistance and it is associated with type 2 diabetes mellitus [9].

Epidemiological, familial and twin studies provide strong evidence for NAFLD heritability [10, 11]. Genetic modifiers of disease severity and progression have been identified through genome-wide association studies [8, 12, 13]. Furthermore, a few large multicentre studies have demonstrated the role of gene variants implicated in insulin signalling, oxidative stress and fibrogenesis in the progression of NAFLD towards NASH and fibrosis [12, 14]. These studies also confirmed the significance of intrahepatocyte fat accumulation and systemic insulin resistance for the progression of liver damage. However, the genetic bases of NAFLD and NASH risk and the relationship with insulin resistance are far from clear.

Pre-B cell leukaemia transcription factor-regulating protein 1 (PREP1) is a homeodomain transcription factor belonging to the TALE family of proteins. This family of proteins also includes the PBX (PBX1–4) and MEIS (MEIS1–3) transcription factors, and plays an important role in haematopoiesis, organogenesis and development. Both PREP and MEIS contain homologous conserved PBX-interacting motifs (HR1 and HR2 domains) and form transcriptionally active complexes with PBX [15–17]. However, while PREP1's main interactor is PBX1, MEIS1 is most involved in interactions with HOX proteins; likewise, while PREP1 acts mainly at promoter sites, MEIS1 acts mainly at promoter-distant sites [18]. As complete *Prep1* (also known as *Pknox1*) knockout is lethal, previous work has shown that *Prep1* hypomorphic heterozygous ($Prep1^{i/+}$) mice feature a complex phenotype characterised by increased insulin sensitivity and protection from streptozotocin-induced diabetes [19]. These animals also feature decreased hepatic triacylglycerol (TG) content, raising the hypothesis that *Prep1* may impact not only on glucose, but also on lipid metabolism in the hepatocyte [20].

In this work, we have addressed this issue and investigated the function of *Prep1* on fatty acid metabolism and TG accumulation in liver. We show that the PREP1/PBX1 complex upregulates transcription of the lipid phosphatase *Ship2* (also known as *Inppl1*), thereby controlling the protein kinase C (PKC)ζ/LKB1/AMPK/ACC signalling cascade, fatty acid synthase (FAS) expression and TG accumulation in liver cells. On the basis of these results, *Prep1* might be considered a new gene involved both in the pathogenesis of insulin resistance and steatohepatitis.

Methods

Materials Media, sera, antibiotics for cell culture and the Lipofectamine reagent were all from Invitrogen (Grand Island, NY, USA). The *pRC/CMV-Prep1*, *pSG5-Pbx1* and $PSG5\text{-}Prep1_{HR1}$ vectors have been previously described [20, 21]. PREP1, actin, PBX1, SH2-containing inositol 5′-phosphatase 2 (SHIP2), pACC, ACC, AMPK, LKB1, calcium/calmodulin-dependent protein kinase kinase β (CAMKKβ), pPKCζ, PKCζ, phosphorylated protein kinase A (pPKA) and PKA antibodies were from Santa Cruz Biotechnology (Santa Cruz, CA, USA). pLKB1, pCAMKKβ and pAMPK antibodies were from Cell Signaling Technology (Beverly, MA, USA). Protein electrophoresis and real-time PCR reagents were from Bio-Rad (Richmond, VA, USA). Western blotting and ECL reagents were from Amersham Biosciences (Arlington Heights, IL, USA). Oil Red O (ORO) stain and all other chemicals were from Sigma (St Louis, MO, USA).

Studies in mice *Prep1*-targeted mice were generated by gene trapping by Lexicon Genetics (The Woodlands, TX, USA). The general phenotype of these mice has been previously described [21–23]. In the experiments reported in this paper, $Prep1^{i/+}$ mice were backcrossed with wild-type (WT)

C57BL/6J mice for generations. All animal handling conformed to regulations of the Ethics Committee on Animal Use of H. S. Raffaele (IACUC permission number 207). The genotyping strategy has been previously described [19].

Hepatic tissue samples were collected rapidly from 8- to 10-week-old male C57BL/6-SV129 mice. Tissues were snap-frozen in liquid nitrogen and stored at −80°C for subsequent western blotting and real-time RT-PCR analysis, as previously described [19].

The blood for serum biochemistry evaluation was collected with an intracardiac method, allowed to clot at room temperature and centrifuged for 10 min; the serum was then separated for shipment. Quantitative analysis of serum TGs was performed with an ABX Pentra400 clinical chemistry analyser using the reagent ABX Pentra Triacylglycerols CP (ABX-Horiba, Montpellier, France) according to the manufacturer's instructions. Serum VLDL-cholesterol and -triacylglycerol levels were measured with ELISA kits (USCN Life Science, Houston, TX, USA).

Methionine- and choline-deficient diet Nine-week-old male C57BL/6-SV129 mice (WT and *Prep1*$^{i/+}$) were divided into four groups. Two groups of mice ($n=9$ WT and $n=9$ *Prep1*$^{i/+}$) were fed a standard rodent chow diet. The other two groups of mice ($n=9$ WT and $n=9$ *Prep1*$^{i/+}$) were fed a methionine- and choline-deficient diet (MCDD). All of the animals were maintained in a temperature- and light-controlled facility, and permitted ad libitum consumption of food and water throughout the 4 weeks of the experimental period. Body weights were measured every week. The animals were killed after overnight fasting for tissue sampling. Blood was collected by cardiac puncture, and the livers were isolated, immediately freeze-clamped in liquid nitrogen and stored at −80°C until analysis. Serum levels of alanine aminotransferase (ALT) and TG were assayed using an ABX Pentra400 clinical chemistry analyser. TG content was extracted from frozen liver tissues and determined as previously described [20].

For the histological examination, livers from killed mice were immediately incised and weighed. Small pieces from each lobe were fixed in 10% formalin and stained with haematoxylin and eosin and ORO for histological analysis. The histological features were grouped into five broad categories: steatosis, inflammation, hepatocellular injury, fibrosis and miscellaneous features. The system of evaluation was adapted from the original proposed by Kleiner et al [24] for the histological evaluation of NASH and took into account the following histological variables: steatosis grade (quantified by low- to medium-power evaluation of parenchymal involvement by steatosis): score 0, <5%; score 1, 5–33%; score 2, >33–66%, score 3, >66%; location (predominant distribution pattern): zone 3, score 0; zone 1, score 1; azonal, score 2; inflammation: lobular inflammation (overall assessment of all inflammatory foci): score 0, no foci; score 1, <2 foci per ×200 field; score 2, 2–4 foci per ×200 field; score 3, >4 foci per ×200 field; necrosis: score 0, present; score 1, absent.

Cell culture procedures and transfection Human hepatocellular carcinoma (HepG2) cells and NMuLi mouse liver cells were cultured at 37°C in DMEM supplemented with 10% FBS, 2% L-glutamine, 10,000 units/ml penicillin and 10,000 μg/ml streptomycin. Transient transfection of *Prep1*, *Prep1*$_{HR1}$ and *Pbx1* plasmids or *Ship2* (5′-GCTCTCTAGTTCCTGCTCCC-3′) phosphorothioate antisense oligonucleotides or *Ship2* (5′-TCGCCACGTCGCTCATTGTT-3′) control scrambled oligonucleotides were performed by the Lipofectamine method according to the manufacturer's instruction (Invitrogen). PREP1 stable clones were selected as previously described [20].

ORO staining To measure cellular neutral lipid droplet accumulation, HepG2 cells were stained by the ORO method as previously described [25].

Western blot analysis Tissue samples were homogenised in a Polytron Homogenizer (Brinkmann Instruments, NY, USA) in 20 ml T-PER reagent (g tissue)$^{-1}$ according to the manufacturer's instructions (Pierce, IL, USA). Total cell lysates were obtained and separated by SDS-PAGE as previously described [26].

Real-time RT-PCR analysis Total cellular RNA was isolated from liver tissue and HepG2 cells using the RNeasy Kit (Qiagen Sciences, Germantown, MD, USA), according to the manufacturer's instructions.

A total of 1 μg of tissue or cell RNA was reverse-transcribed using SuperScript II Reverse Transcriptase (Invitrogen). PCR reactions were analysed using SYBR Green mix (Bio-Rad, Hercules, CA, USA). Reactions were performed using the Platinum SYBR Green qPCR SuperMix-UDG using an iCycler IQ Multi-Color Real Time PCR Detection System (Bio-Rad). All reactions were performed in triplicate and β-actin was used as an internal standard. The primer sequences used are described in electronic supplementary material (ESM) Table 1.

Chromatin immunoprecipitation and luciferase assays Chromatin immunoprecipitation (ChIP) and re-ChIP assays were performed using NMuLi cells as previously described [27]. For luciferase assays, the mouse *Ship2* fragment −1,385 bp to −1,115 bp was amplified by PCR from genomic mouse DNA isolated from the murine liver cell line (NMuLi cells). The following primers were used: forward: 5′-KpnI-CAAAGGGGAAGCTGGAAACGGGA-3′ and reverse: 5′-XhoI-TTAGCCGAAGGCTAGAGGGTGCT-3′, where KpnI and XhoI indicate the restriction sites added to the sequence. The amplified fragments were cloned in the pGL3

promoter vector (Promega, Madison, WI, USA) by KpnI and XhoI. NMuLi cells were cotransfected with 2 μg of *Ship2* promoter vector together with different amounts of *Prep1* and *Pbx1* expression vectors. Total DNA content (up to 4 μg/plate) was normalised to the empty vector devoid of *Prep1* and *Pbx1* coding sequence. Forty-eight hours after transfection the cells were harvested and lysed as described previously [27]. Luciferase activity was measured by a commercial luciferase assay kit (Promega). Values were normalised for beta-galactosidase.

Statistical procedures Data were analysed with StatView software (Abacus Concepts, Piscataway, NJ, USA) by two-factor ANOVA. p values of <0.05 were considered statistically significant [28].

Results

Prep1 impact on lipogenesis-controlling signalling events in mouse liver Serum TG content, but not hepatic *ApoB100* (also known as *Apob*) expression or serum VLDL secretion, was reduced by 33% in *Prep1*$^{i/+}$ mice compared with their non-hypomorphic littermates (WT) (Fig. 1a–c). *Fas* expression decreased by 65% in *Prep1*$^{i/+}$ compared with WT mice, while *Acc* and *Srebp-1c* (encoding sterol regulatory element binding protein-1c) were not significantly affected in *Prep1*$^{i/+}$ mice (Fig. 1d). To investigate this issue in greater detail, we first focused our attention on one of the major lipogenesis regulatory enzymes, AMPK, and on its downstream target, ACC. Active AMPK, phosphorylated at Thr172, was significantly upregulated in *Prep1*$^{i/+}$ mice, with no change in AMPK protein levels. Indeed, the pAMPK to AMPK ratio was threefold higher in *Prep1*$^{i/+}$ compared with WT mice. The expression and phosphorylation of ACC at Ser79 closely matched those of AMPK (Fig. 2a). We next examined the upstream signalling mechanisms converging on AMPK and assayed phosphorylation of both LKB1 and CAMKKβ. As shown in Fig. 2b, LKB1exhibited almost threefold increased phosphorylation in *Prep1*$^{i/+}$ mice, while CAMKKβ exhibited no difference between *Prep1*$^{i/+}$ and WT mice.

Several protein kinases play a major role in transducing regulatory signals to LKB1 [29, 30]. In particular, atypical PKCζ and PKA have been reported to represent major LKB1 regulators. In our *Prep1*$^{i/+}$ mice only PKCζ exhibited

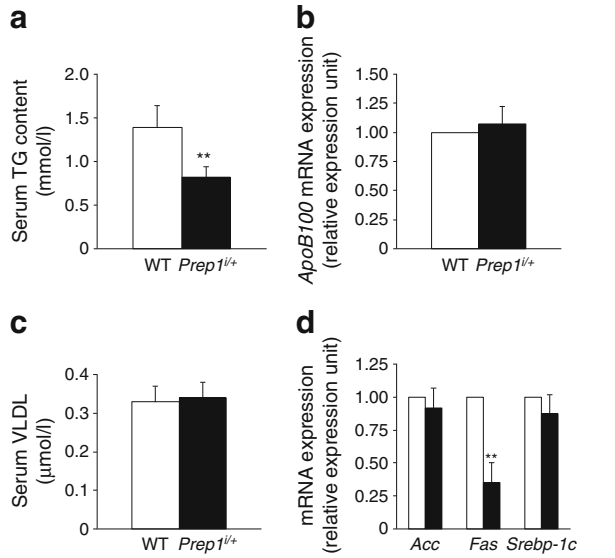

Fig. 1 Serum TG and VLDL content and *Fas* mRNA levels in *Prep1*$^{i/+}$ mice. (**a**) Serum TG content was measured as described in the Methods. Each bar represents the mean±SD of three independent experiments in triplicate (eight mice/genotype). (**b**) Hepatic levels of *ApoB100* mRNA were quantified by real-time RT-PCR analysis, using β-actin as the internal standard. (**c**) Serum VLDL was measured by ELISA assay, as described in the Methods. Each bar represents the mean±SD of three independent experiments in triplicate (eight mice/genotype). (**d**) The abundance of *Acc*, *Fas* and *Srebp-1c* mRNA was determined by real-time RT-PCR analysis of total RNA isolated from the liver of *Prep1*$^{i/+}$ (black bars) and control mice (white bars), using β-actin as the internal standard. (**b**, **d**) Bars represent the mean±SD of four independent experiments, in each of which the reactions were performed in triplicate using the pooled total RNAs obtained from six mice/genotype. $^{**}p<0.01$

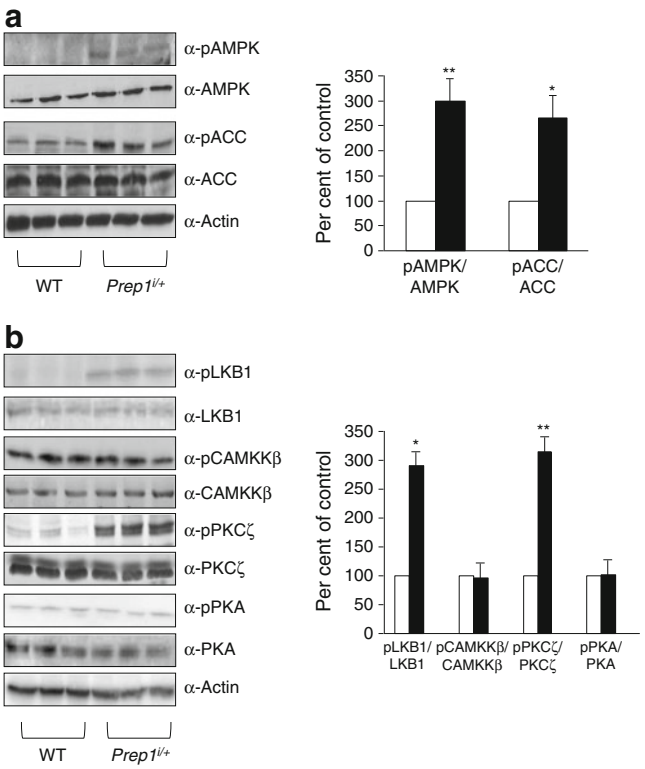

Fig. 2 AMPK signalling in *Prep1*$^{i/+}$ mice. (**a**) Liver tissue from *Prep1*$^{i/+}$ (black bars) and control mice (white bars) was dissected and solubilised, and protein samples were analysed by western blot with pAMPK, AMPK, pACC and ACC antibodies. (**b**) Aliquots of the lysates were also blotted with pLKB1, LKB1, pCAMKKβ, CAMKKβ, pPKCζ, PKCζ, pPKA and PKA antibodies. Actin antibody was used for normalisation. The blots shown are representative of four independent experiments. Bars represent the mean±SD of densitometric values from the four experiments. $^{*}p<0.05$, $^{**}p<0.01$

enhanced phosphorylation, as phosphorylation of PKA was very comparable in *Prep1*$^{i/+}$ and WT mice (Fig. 2b).

To further explore the impact of PREP1 on hepatic lipogenesis, we transiently transfected *Prep1* cDNA in HepG2 cells (Fig. 3a). We then analysed the lipid accumulation in these cells by ORO staining. As shown in Fig. 3b, ORO staining was twofold higher in *Prep1*-overexpressing cells than in controls transfected with an empty vector. *Fas*, but not *Acc*, mRNA levels also increased by 50% in the *Prep1*-transfected cells (Fig. 3c), while phosphorylation of PKCζ, LKB1, AMPK and ACC was significantly reduced (Fig. 3d).

Prep1 regulates hepatic lipogenesis via Ship2 PREP1 regulation of hepatic gluconeogenesis occurs through a PREP1/PBX1 complex [20]. We therefore hypothesised that PBX1 co-regulates the PREP1 action on lipogenesis. To examine this possibility, we transfected HepG2 cells with either *Pbx1* or *Prep1*$_{HR1}$ cDNA. The latter is unable to bind and form a complex with PBX1 [21]. Similarly to PREP1, PBX1 was found to downregulate the PKCζ/LKB1/AMPK/ACC phosphorylation cascade and induce *Fas* expression and intracellular lipid droplet accumulation in the liver cells. In contrast, *Prep1*$_{HR1}$ transfection elicited no effect on these mechanisms, indicating that PBX1 binding is necessary for PREP1 control of lipogenesis (ESM Fig. 1).

Published evidence indicates that the lipid phosphatase SHIP2 reduces cellular levels of phosphatidylinositol-3-kinase-generated phosphatidylinositol-3-phosphate and PKCζ activation [31–33]. Interestingly, SHIP2 protein and mRNA levels in the livers of *Prep1*$^{i/+}$ mice were reduced by more than 60% compared with WT (Fig. 4a, b). Transfection of either *Prep1* or *Pbx1* cDNAs in HepG2 cells induced a close to twofold increase in SHIP2 protein and mRNA expression, while transfection of the *Prep1*$_{HR1}$ mutant caused no change (Fig. 4c, d). We therefore used *Ship2*-specific antisense oligonucleotides to test the hypothesis that SHIP2 represents a downstream mediator of the PREP1/PBX1 action on hepatic lipogenesis. Indeed, transfection of *Ship2*-specific antisense oligonucleotides in HepG2$_{PREP1c}$ cells (which overexpress *Prep1* by fivefold) [20] caused a 75% reduction in SHIP2 levels and, in parallel, generated a phenotype similar to that observed in *Prep1*$^{i/+}$ mice, with a more than fourfold increase in AMPK and ACC phosphorylation and downregulated *Fas*, but not *Acc*, expression (Fig. 5). PKCζ and LKB1 phosphorylation was also significantly induced in *Ship2*-specific antisense oligonucleotide transfected cells (data not shown).

Prep1 regulation of Ship2 gene transcription Bioinformatic analysis revealed the presence of a potential PREP1/PBX1 binding site at position −1,284 to −1,268 upstream of the transcription initiation site of the *Ship2* gene (Fig. 6a). To validate this putative region, we used specific antibodies against either PREP1 or PBX1 and performed ChIP and re-ChIP studies in NMuLi mouse liver cells. These experiments revealed the simultaneous presence of both Prep1 and Pbx1 at the putative binding site (Fig. 6b). We than cloned the PREP1/PBX1 binding fragment into a pGL3 promoter construct upstream of the luciferase gene. This construct was then cotransfected into NMuLi cells together with *Prep1*, *Pbx1*, both the transcription factors and *Prep1*$_{HR1}$ cDNAs, followed

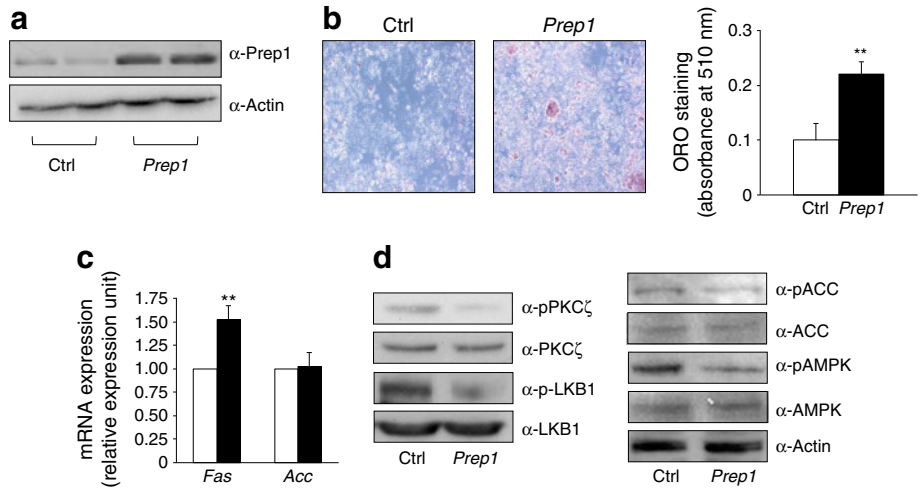

Fig. 3 Effect of the overexpression of *Prep1* on TG accumulation, *Fas* expression and AMPK signalling in HepG2 cells. (**a**) HepG2 cells were transiently transfected with *Prep1* cDNA. The cells were then solubilised and lysates analysed by immunoblotting with PREP1 antibodies to verify the transfection. Actin antibodies were used for normalisation. The blot shown is representative of four different experiments. (**b**) HepG2 cells were stained with ORO as described in the Methods. The photograph shown is representative of five independent experiments. (**c**) The levels of *Fas* and *Acc* mRNA in cells transfected with *Prep1* cDNA (black bars) or in control cells transfected with an empty vector (white bars) were quantified by real-time RT-PCR analysis, using β-actin as the internal standard. Bars represent the mean±SD of four independent experiments. $^{**}p<0.01$. (**d**) HepG2 cell lysates were western blotted with pPKCζ, PKCζ, pLKB1, LKB1, pACC, ACC, pAMPK or AMPK antibodies, as outlined in the legend to Fig. 2. The blots shown are representative of four independent experiments. Ctrl, control

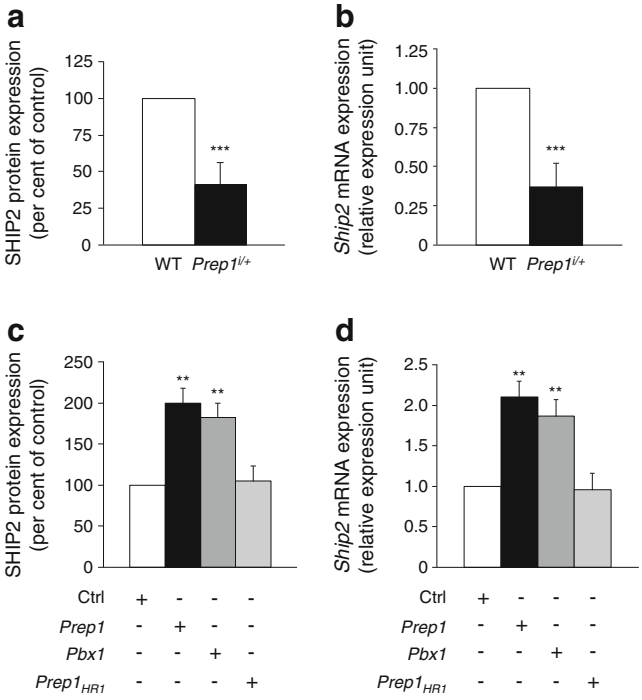

Fig. 4 *Ship2* expression in *Prep1*$^{i/+}$ mice and in *HepG2*-overexpressing PREP1. (**a**) SHIP2 protein abundance was analysed by western blotting lysates of hepatic tissue from *Prep1*$^{i/+}$ and control mice using specific antibodies. Actin antibodies were used for normalisation. Each bar represents the mean±SD of duplicate determinations in ten mice/group. (**b**) The abundance of *Ship2* mRNA was determined by real-time RT-PCR analysis of total RNA isolated from the liver of *Prep1*$^{i/+}$ and control mice, using β-actin as the internal standard. Bars represent the mean±SD of five independent experiments, each of which were performed in triplicate using the pooled total RNAs obtained from six mice/genotype. (**c**) Lysates from control or overexpressing *Prep1*, *Pbx1* and *Prep1*$_{HR1}$ cDNAs HepG2 cells were blotted with SHIP2 antibodies. Actin antibodies were used for normalisation. Each bar represents the mean±SD of duplicate determinations from four independent experiments. (**d**) The levels of *Ship2* mRNA in cells transfected as described above were quantified by real-time RT-PCR analysis, using β-actin as the internal standard. Each bar represents the mean±SD of duplicate determinations from four independent experiments. $^{**}p<0.01$, $^{***}p<0.001$. Ctrl, control

by measurement of luciferase activity. As shown in Fig. 6c, *Prep1* and *Pbx1* enhanced luciferase activity by 17-fold, while *Prep1*$_{HR1}$ did not elicit any effect.

Prep1$^{i/+}$ *mice are resistant to diet-induced steatohepatitis* To assess the in vivo significance of PREP1 control of hepatic lipogenesis, we analysed the effect of a steatogenic MCDD in *Prep1*$^{i/+}$ mice. After 4 weeks of the MCDD, both *Prep1*$^{i/+}$ mice and their non-hypomorphic littermates showed significant weight loss (Table 1), which was independent of food intake (data not shown). Liver weight also comparably decreased in both of the mice groups upon diet administration. Both serum ALT and TG levels were lower in the *Prep1*$^{i/+}$ mice at baseline. Interestingly, the increase in ALT levels and decrease in TG levels following the regimen was significantly less pronounced in *Prep1*$^{i/+}$ compared with control mice. In addition, MCDD-induced accumulation of TGs was 25% reduced in *Prep1*$^{i/+}$ mouse liver (Fig. 7a). Indeed, livers from MCDD-fed WT mice revealed very significant morphological evidence of steatosis (score 2–3) accompanied by severe lobular inflammation (score 2–3) and foci of necrosis (Fig. 7b) as indicated by the arrows. In comparison, *Prep1*$^{i/+}$ mice showed only grade 1 hepatic steatosis, grade 0–1 inflammation and absence of necrosis. In addition, little ORO staining accumulation occurred in these mice in comparison with their non-hypomorphic littermates. When fed a regular chow diet, these animals showed no histological differences in livers, suggesting that PREP1 expression levels determine the hepatocyte sensitivity to a steatogenic diet.

Discussion

NAFLD spans from steatosis to NASH, with lobular inflammatory and necrotic lesions and fibrosis [34]. Metabolic abnormalities, including dysregulated insulin signalling and action, and nutritional and genetic factors are well-established contributors to the onset and progression of these liver disorders [7]. Indeed, patients with insulin resistance syndrome have a four- to eleven-fold increased risk of developing NAFLD [9]. In addition, small-interfering-RNA-mediated suppression of IRS1 and IRS2 results in hepatic insulin resistance, glucose intolerance and hepatic steatosis in rodents [35, 36]. However, the identity of the genes affecting the risk of NAFLD and of NASH as well as the molecular mechanisms involved in their function have been only partially uncovered.

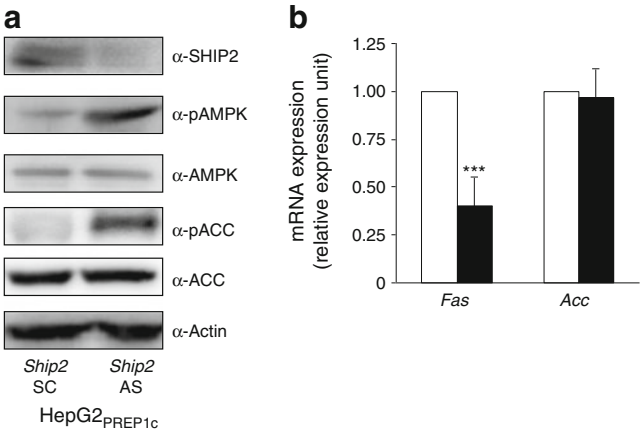

Fig. 5 Effect of *Ship2* antisense on lipogenesis regulation in PREP1-transfected HepG2 cells. (**a**) HepG2$_{PREP1c}$ cells were transfected with specific *Ship2* phosphorothioate antisense oligonucleotides (*Ship2* AS) or scrambled oligonucleotides (*Ship2* SC) and analysed by western blot with SHIP2, pAMPK, AMPK, pACC, ACC or actin antibodies. The blots shown are representative of four independent experiments. (**b**) The levels of *Fas* and *Acc* mRNA in HepG2$_{PREP1c}$ transfected with *Ship2* AS (black bars) or a *Ship2* SC (white bars) were quantified by real-time RT-PCR analysis, using β-actin as the internal standard. Bars represent the mean ± SD of four independent experiments. $^{***}p<0.001$

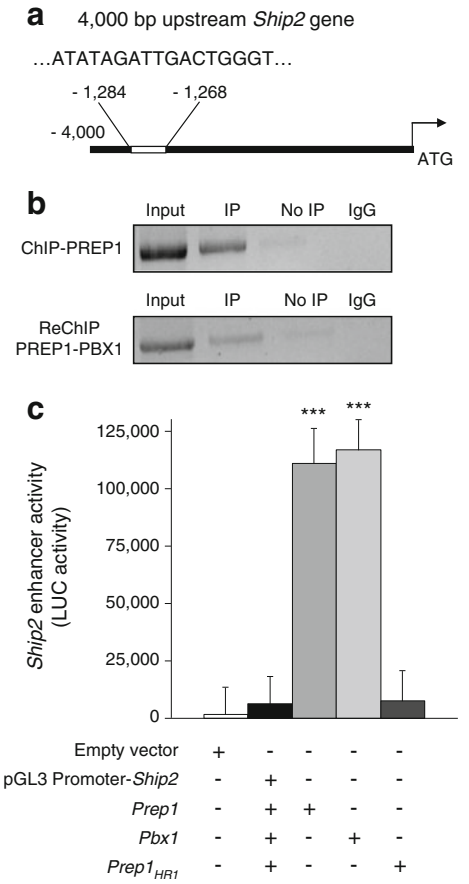

Fig. 6 PREP1/PBX1 regulation of *Ship2* reporter gene activity. (**a**) Schematic representation of the 5′ sequence upstream of the putative *Ship2* transcription start site with the potential binding site for PREP1 and PBX1. (**b**) Soluble chromatin was prepared from NMuLi mouse liver cells and immunoprecipitated with PREP1 antibodies. Total (input) and immunoprecipitated DNAs were amplified using primer pairs encompassing the indicated *Ship2* fragments. A re-ChIP assay with PBX1 antibodies was performed as described in the Methods. (**c**) NMuLi cells were transfected with 2 μg of the *Ship2* enhancer–luciferase construct alone or in combination with *Prep1*, *Pbx1* or the mutant $Prep1_{HR1}$. Luciferase (LUC) activity was assayed and normalised as described in the Methods. Bars represent mean values±SD of determinations from four independent experiments. ***$p<0.001$

Previous work in our laboratory revealed that PREP1 attenuates insulin glucoregulatory function in liver by transcriptional activation of the *Shp1* (also known as *Ptpn6*) gene, a known silencer of insulin signalling [20]. In addition, we showed that $Prep1^{i/+}$ mice feature reduced hepatic TG content. In the present work, we demonstrate that these mice also exhibit depressed serum TG levels. This effect is not due to changes in VLDL secretion or in hepatic *ApoB100* expression, which are required for TG transport in plasma [37]. However, we found that the reduced serum TG level featured by the $Prep1^{i/+}$ mice was accompanied by reduced *Fas* expression, prompting us to explore the hypothesis that PREP1 also controls hepatic lipid synthesis. Indeed, we have shown that, in livers from $Prep1^{i/+}$ mice, the major inhibitor of de novo lipogenesis, AMPK, was strongly induced, accompanied by an increase in ACC phosphorylation. AMPK regulates hepatic lipid metabolism by exerting short- and long-term effects. Short-term regulation includes AMPK phosphorylation and inactivation of ACC, thereby inhibiting fatty acid biosynthesis. Long-term effects include AMPK regulation of lipogenesis by inhibition of SREBP-1c and promotion of lipogenic gene expression, such as *Acc* and *Fas* [3]. Because *Srebp-1c* and *Acc* expression were not reduced in $Prep1^{i/+}$ mice, the short-term effects of AMPK might have prevailed in these $Prep1^{i/+}$ mice. Indeed, PKCζ/LKB1 signalling was also induced in *Prep1*-deficient mouse liver. Work by Luna and co-workers has demonstrated that metformin-induced activation of AMPK is accompanied by induction of PKCζ [38]. Importantly, genetic ablation as well as pharmacologic inhibition of PKCζ prevent stimulation of both LKB1 and AMPK [29], indicating that PREP1 lipogenic signalling upstream of AMPK involves PKCζ upregulation. Consistent with this mechanism, we show that *Prep1* overexpression in liver cells downregulates PKCζ function and AMPK activity and enhances lipid accumulation. Previous work in our laboratory demonstrated that *Prep1* silencing enhances liver insulin sensitivity and insulin-dependent glycogen synthesis [20]. In contrast, lipogenesis was downregulated in the $Prep1^{i/+}$ mice. Downregulation of lipogenesis might be independent of and prevailing on the enhanced insulin sensitivity caused by *Prep1* silencing. In addition, the increased liver sensitivity to insulin might be confined to glycogen synthesis and not present in other pathways.

In vivo, genetic ablation of the inositol phosphate phosphatase SHIP2 determines a phenotype reminiscent of that of

Table 1 Characterisation of WT and $Prep1^{i/+}$ mice

Variable	Control diet		MCDD	
	WT	$Prep1^{i/+}$	WT	$Prep1^{i/+}$
Initial body weight (g)	28.7±1.0	25.5±0.6	28±0.12	27.2±0.5
Final body weight (g)	30.4±0.9	30.1±0.4	19.1±0.7*	18.8±1.0***
Liver weight (g)	1.16±0.9	1.06±0.5	0.86±0.5*	0.81±0.4*
Serum ALT level (μkat/l)	1.47±0.11	1.09±0.1	5.13±0.1**	2.59±0.01**††
Serum TG level (mmol/l)	1.18±0.05	0.85±0.03†	0.87±0.04*	0.68±0.05*†

Values are means±SD

*$p<0.05$; **$p<0.01$; ***$p<0.001$ for differences between animals fed an MCDD vs control diet

†$p<0.05$; ††$p<0.01$ for differences between $Prep1^{i/+}$ vs WT mice

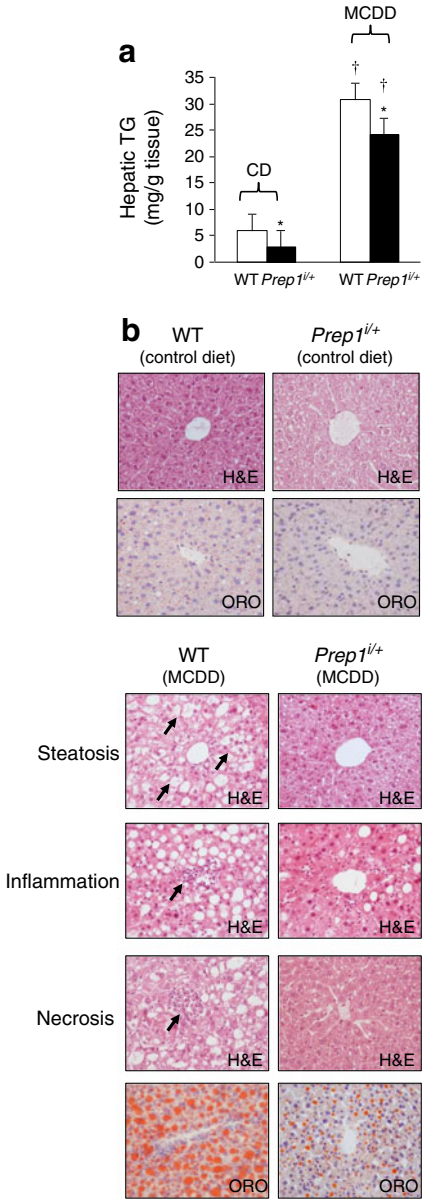

Fig. 7 Effect of the MCDD on *Prep1*$^{i/+}$ mice. (**a**) *Prep1*$^{i/+}$ and control mice (nine mice/group) were fed an MCDD or control diet (CD) and intrahepatic TG content was measured as described in the Methods. Bars represent the means±SD of values obtained from each group of animals. *$p<0.05$, MCDD vs CD; $^{\dagger}p<0.05$, *Prep1*$^{i/+}$ vs WT mice. (**b**) Representative liver histology of WT and *Prep1*$^{i/+}$ mice fed a control diet and MCDD. Liver sections were stained with haematoxylin and eosin (H&E) or ORO and examined by light microscopy with a magnification of ×40; arrows show foci of steatosis, inflammation and necrosis

Prep1$^{i/+}$ mice. First, both *Ship2*-null mice and *Prep1*$^{i/+}$ mice feature enhanced peripheral sensitivity to insulin [39]. Second, serum TG levels are significantly reduced in both of these genetic models [39], raising the possibility that, at least in part, the *Prep1*$^{i/+}$ mouse phenotype is determined by reduced *Ship2* expression and/or function. This proved to be correct, as *Ship2* mRNA as well as protein levels were found to be strongly reduced in the livers of *Prep1*$^{i/+}$ mice, while the opposite changes occurred in liver cells transfected with *Prep1* cDNA. Of importance, antisense silencing of *Ship2* in hepatocytes prevents signalling activation through the PKCζ/LKB1/AMPK cascade and *Fas* induction caused by PREP1 overexpression. These findings indicate that the *Ship2* gene represents a transcriptional target of PREP1, upstream of the AMPK control of hepatic lipogenesis. The SHP1 and SHP2 tyrosine phosphatases are also upregulated by PREP1 [20]. Both of these phosphatases may silence PKCζ by attenuating insulin signalling in cells expressing increased levels of *Prep1*. In addition, recent work by Nagata and co-workers revealed that liver-specific ablation of SHP2 protects mice from developing liver steatosis [40]. However, antisense silencing of SHP1, SHP2 or both of these phosphatases in liver cells has negligible effects on the increased TG synthesis caused by PREP1 overexpression (data not shown), indicating a marginal, if any, role in PREP1 control of liver lipogenesis.

The mechanistic details involved in PREP1 control of SHIP2 function and the hypothesis that they may include direct transcriptional regulation are addressed in the present paper. We first identified a putative PREP1 binding site in the *Ship2* regulatory region upstream of the transcription initiation site of the gene. Subsequent ChIP experiments demonstrated PREP1 binding to this putative site. In addition, we have shown that this binding enhances *Ship2* reporter activity in luciferase assays. These results are also supported by the analysis of ChIP-sequencing experiments performed on human A549 cells overexpressing PREP1, which identified a weak PREP1 binding site about 1.3 kb upstream of the *Ship2* transcription start site. Moreover, in NIH 3T3-L1 pre-adipocytes, the downregulation of *Prep1* induces the loss of the H3K4Me1 chromatin mark, which is specific for enhancers; this effect is not generalised to other genes (data not shown).

Further ChIP/re-ChIP experiments revealed the simultaneous presence of the major PREP1 co-regulatory factor PBX1 [15] at the *Ship2* promoter. We showed that PBX1 is required for PREP1 regulation of lipogenesis since: (1) PBX1 mimics PREP1 signalling through the SHIP2/PKCζ/LKB1/AMPK/ACC cascade; and (2) expression of the PREP1$_{HR1}$ mutant, which is unable to bind PBX1, prevents PBX1 recruitment at the *Ship2* promoter and, simultaneously, prevents the induction of lipogenic signalling. Previous studies in liver have demonstrated that PREP1 controls insulin glucoregulatory function by transcriptional targeting of the *Shp1* tyrosine phosphatase [20]. As in the case of lipogenesis, overexpression of PBX1 mimics PREP1 action on glucose homeostasis. Thus, in the liver, transcriptional targeting of both lipid and tyrosine phosphatases occurs in partnership with PBX1.

An MCDD results in liver injury similar to human NASH [41]. In addition to increased fatty acid uptake and decreased VLDL secretion, enhanced lipogenesis contributes to the hepatic accumulation of TGs in livers of MCDD-treated mice [42]. Similar mechanisms may predispose to hepatocyte

damage in human NASH [43]. However, the molecular and genetic mechanisms responsible for NASH have been only partially uncovered. In the present report, we show that silencing of the *Prep1* gene protects mice from the TG accumulation and hepatocyte damage caused by MCDD administration, indicating that PREP1 may represent a molecular link between insulin resistance and the development of hepatic steatosis. Whether PREP1 itself or nearby loci affect lipid metabolism or are implicated in NAFLD in humans remains to be clarified. Current evidence indicates that PREP1 expression is increased in patients with alcoholic steatohepatitis, supporting the hypothesis that PREP1 may also have a role in humans [44].

Funding This work was supported by the European Foundation for the Study of Diabetes, the European Commission's PREPOBEDIA project (201681) and the Ministero dell'Università e della Ricerca Scientifica (PRIN and FIRB: RBIP0689BS). The financial support of Telethon–Italy to FBe and FBl is also gratefully acknowledged.

Duality of interest The authors declare that there is no duality of interest associated with this manuscript.

Contribution statement FO and SC were the main contributors in terms of conception, design, acquisition and interpretation of data and drafting the article. AL, ML, LP, TBP, GAR, DP, OP and CM contributed to conceptual design and the acquisition of data. PF and FBl contributed to conceptual design, analysis and interpretation of data and discussion of the results. FBe contributed to conceptual design, interpretation and discussion of the results and supervision of the overall work. All of the authors critically revised the article and approved the final version.

References

1. Postic C, Dentin R, Girard J (2004) Role of the liver in the control of carbohydrate and lipid homeostasis. Diabetes Metab 30:398–408
2. Witters LA, Kemp BE (1992) Insulin activation of acetyl-CoA carboxylase accompanied by inhibition of the 5′-AMP-activated protein kinase. J Biol Chem 267:2864–2867
3. Viollet B, Foretz M, Guigas B et al (2006) Activation of AMP-activated protein kinase in the liver: a new strategy for the management of metabolic hepatic disorders. J Physiol 574:41–53
4. Towler MC, Hardie DG (2007) AMP-activated protein kinase in metabolic control and insulin signaling. Circ Res 100:328–341
5. Carling D (2004) The AMP-activated protein kinase cascade—a unifying system for energy control. Trends Biochem Sci 29:18–24
6. Shackelford DB, Shaw RJ (2009) The LKB1-AMPK pathway: metabolism and growth control in tumour suppression. Nat Rev Cancer 9:563–575
7. Di Rosa M, Malaguarnera L (2012) Genetic variants in candidate genes influencing NAFLD progression. J Mol Med 90:105–118
8. Dongiovanni P, Anstee QM, Valenti L (2013) Genetic predisposition in NAFLD and NASH: impact on severity of liver disease and response to treatment. Curr Pharm Des 19:5219–5238
9. Nagle CA, Klett EL, Coleman RA (2009) Hepatic triacylglycerol accumulation and insulin resistance. J Lipid Res 50(Suppl):S74–S79
10. Struben VM, Hespenheide EE, Caldwell SH (2000) Nonalcoholic steatohepatitis and cryptogenic cirrhosis within kindreds. Am J Med 108:9–13
11. Willner IR, Waters B, Patil SR, Reuben A, Morelli J, Riely CA (2001) Ninety patients with nonalcoholic steatohepatitis: insulin resistance, familial tendency, and severity of disease. Am J Gastroenterol 96: 2957–2961
12. Anstee QM, Daly AK, Day CP (2011) Genetic modifiers of non-alcoholic fatty liver disease progression. Biochim Biophys Acta 1812:1557–1566
13. Guichelaar M, Gawrieh S, Olivier M et al (2013) Interactions of allelic variance of PNPLA3 with non genetic factors in predicting NASH and non-hepatic complications of severe obesity. Obesity. doi: 10.1002/oby.20327
14. Al-Serri A, Anstee QM, Valenti L et al (2012) The SOD2 C47T polymorphism influences NAFLD fibrosis severity: evidence from case-control and intra-familial allele association studies. J Hepatol 56:448–454
15. Berthelsen J, Zappavigna V, Ferretti E, Mavilio F, Blasi F (1998) The novel homeoprotein Prep1 modulates Pbx-Hox protein cooperativity. EMBO J 17:1434–1445
16. Berthelsen J, Kilstrup-Nielsen C, Blasi F, Mavilio F, Zappavigna V (1999) The subcellular localization of PBX1 and EXD proteins depends on nuclear import and export signals and is modulated by association with PREP1 and HTH. Genes Dev 13:946–953
17. Berthelsen J, Zappavigna V, Mavilio F, Blasi F (1998) Prep1, a novel functional partner of Pbx proteins. EMBO J 17:1423–1433
18. Penkov D, Mateos San Martin D, Fernandez-Diaz LC et al (2013) Analysis of the DNA-binding profile and function of TALE homeoproteins reveals their specialization and specific interactions with Hox genes/proteins. Cell Rep 3:1321–1333
19. Oriente F, Fernandez Diaz LC, Miele C et al (2008) Prep1 deficiency induces protection from diabetes and increased insulin sensitivity through a p160-mediated mechanism. Mol Cell Biol 28:5634–5645
20. Oriente F, Iovino S, Cabaro S et al (2011) Prep1 controls insulin glucoregulatory function in liver by transcriptional targeting of SHP1 tyrosine phosphatase. Diabetes 60:138–147
21. Diaz VM, Mori S, Longobardi E et al (2007) p160 Myb-binding protein interacts with Prep1 and inhibits its transcriptional activity. Mol Cell Biol 27:7981–7990
22. Penkov D, Di Rosa P, Fernandez Diaz L et al (2005) Involvement of Prep1 in the alphabeta T cell receptor T-lymphocytic potential of hematopoietic precursors. Mol Cell Biol 25:10768–10781
23. Ferretti E, Villaescusa JC, Di Rosa P et al (2006) Hypomorphic mutation of the TALE gene Prep1 (pKnox1) causes a major reduction of Pbx and Meis proteins and a pleiotropic embryonic phenotype. Mol Cell Biol 26:5650–5662
24. Kleiner DE, Brunt EM, van Natta M et al (2005) Design and validation of a histological scoring system for nonalcoholic fatty liver disease. Hepatology 41:1313–1321
25. Ramirez-Zacarias JL, Castro-Munozledo F, Kuri-Harcuch W (1992) Quantitation of adipose conversion and triglycerides by staining intracytoplasmic lipids with Oil Red O. Histochemistry 97:493–497
26. Miele C, Caruso M, Calleja V et al (1999) Differential role of insulin receptor substrate (IRS)-1 and IRS-2 in L6 skeletal muscle cells expressing the Arg1152 --> Gln insulin receptor. J Biol Chem 274: 3094–3102
27. Ungaro P, Teperino R, Mirra P et al (2008) Molecular cloning and characterization of the human PED/PEA-15 gene promoter reveal antagonistic regulation by hepatocyte nuclear factor 4alpha and chicken ovalbumin upstream promoter transcription factor II. J Biol Chem 283:30970–30979
28. Vigliotta G, Miele C, Santopietro S et al (2004) Overexpression of the ped/pea-15 gene causes diabetes by impairing glucose-stimulated insulin secretion in addition to insulin action. Mol Cell Biol 24:5005–5015
29. Xie Z, Dong Y, Scholz R, Neumann D, Zou MH (2008) Phosphorylation of LKB1 at serine 428 by protein kinase C-zeta is required for metformin-enhanced activation of the AMP-activated protein kinase in endothelial cells. Circulation 117:952–962
30. Song P, Xie Z, Wu Y, Xu J, Dong Y, Zou MH (2008) Protein kinase Czeta-dependent LKB1 serine 428 phosphorylation increases LKB1

nucleus export and apoptosis in endothelial cells. J Biol Chem 283: 12446–12455
31. Hori H, Sasaoka T, Ishihara H et al (2002) Association of SH2-containing inositol phosphatase 2 with the insulin resistance of diabetic db/db mice. Diabetes 51:2387–2394
32. Sasaoka T, Wada T, Tsuneki H (2006) Lipid phosphatases as a possible therapeutic target in cases of type 2 diabetes and obesity. Pharmacol Ther 112:799–809
33. Wada T, Sasaoka T, Funaki M et al (2001) Overexpression of SH2-containing inositol phosphatase 2 results in negative regulation of insulin-induced metabolic actions in 3T3-L1 adipocytes via its 5′-phosphatase catalytic activity. Mol Cell Biol 21:1633–1646
34. Angulo P (2002) Nonalcoholic fatty liver disease. N Engl J Med 346: 1221–1231
35. Taniguchi CM, Ueki K, Kahn R (2005) Complementary roles of IRS-1 and IRS-2 in the hepatic regulation of metabolism. J Clin Invest 115:718–727
36. Farese RV Jr, Zechner R, Newgard CB, Walther TC (2012) The problem of establishing relationships between hepatic steatosis and hepatic insulin resistance. Cell Metab 15:570–573
37. Mason TM (1998) The role of factors that regulate the synthesis and secretion of very-low-density lipoprotein by hepatocytes. Crit Rev Clin Lab Sci 35:461–487
38. Luna V, Casauban L, Sajan MP et al (2006) Metformin improves atypical protein kinase C activation by insulin and phosphatidylinositol-3,4,5-(PO4)3 in muscle of diabetic subjects. Diabetologia 49:375–382
39. Sleeman MW, Wortley KE, Lai KM et al (2005) Absence of the lipid phosphatase SHIP2 confers resistance to dietary obesity. Nat Med 11: 199–205
40. Nagata N, Matsuo K, Bettaieb A et al (2012) Hepatic Src homology phosphatase 2 regulates energy balance in mice. Endocrinology 153: 3158–3169
41. Rinella ME, Elias MS, Smolak RR, Fu T, Borensztajn J, Green RM (2008) Mechanisms of hepatic steatosis in mice fed a lipogenic methionine choline-deficient diet. J Lipid Res 49:1068–1076
42. Pickens MK, Yan JS, Ng RK et al (2009) Dietary sucrose is essential to the development of liver injury in the methionine-choline-deficient model of steatohepatitis. J Lipid Res 50:2072–2082
43. Macfarlane DP, Zou X, Andrew R et al (2011) Metabolic pathways promoting intrahepatic fatty acid accumulation in methionine and choline deficiency: implications for the pathogenesis of steatohepatitis. Am J Physiol Endocrinol Metab 300:E402–E409
44. Affò S, Dominguez M, Lozano JJ et al (2013) Transcriptome analysis identifies TNF superfamily receptors as potential therapeutic targets in alcoholic hepatitis. Gut 62:452–460